LABORATORI NAZIONALI DI FRASCATI
SIS-Pubblicazioni

A Theoretical Reappraisal of Branching Ratios and CP Asymmetries in the Decays $B \to (X_d, X_s)\ell^+\ell^-$ and Determination of the CKM Parameters

Ahmed Ali[1], Gudrun Hiller[2]

[1] *Deutsches Elektronen-Synchrotron DESY, Hamburg, FRG*

[2] *INFN, Laboratori Nazionali di Frascati, P.O. Box 13, I-00044 Frascati, Italy*

Abstract

We present a theoretical reappraisal of the branching ratios and CP asymmetries for the decays $B \to X_q \ell^+\ell^-$, with $q = d, s$, taking into account current theoretical uncertainties in the description of the inclusive decay amplitudes from the long-distance contributions, an improved treatment of the renormalization scale dependence, and other parametric dependencies. Concentrating on the partial branching ratios $\Delta\mathcal{B}(B \to X_q \ell^+\ell^-)$, integrated over the invariant dilepton mass region $1 \text{ GeV}^2 \leq s \leq 6 \text{ GeV}^2$, we calculate theoretical precision on the charge-conjugate averaged partial branching ratios $\langle\Delta\mathcal{B}_q\rangle = (\Delta\mathcal{B}(B \to X_q \ell^+\ell^-) + \Delta\mathcal{B}(\bar{B} \to \bar{X}_q \ell^+\ell^-))/2$, CP asymmetries in partial decay rates $(a_{CP})_q = (\Delta\mathcal{B}(B \to X_q \ell^+\ell^-) - \Delta\mathcal{B}(\bar{B} \to \bar{X}_q \ell^+\ell^-))/(2\langle\Delta\mathcal{B}_q\rangle)$, and the ratio of the branching ratios $\Delta\mathcal{R} = \langle\Delta\mathcal{B}_d\rangle/\langle\Delta\mathcal{B}_s\rangle$. For the central values of the CKM parameters, we find $\langle\Delta\mathcal{B}_s\rangle = (2.22^{+0.29}_{-0.30}) \times 10^{-6}$, $\langle\Delta\mathcal{B}_d\rangle = (9.61^{+1.32}_{-1.47}) \times 10^{-8}$, $(a_{CP})_s = -(0.19^{+0.17}_{-0.19})\%$, $(a_{CP})_d = (4.40^{+3.87}_{-4.46})\%$, and $\Delta\mathcal{R} = (4.32 \pm 0.03)\%$. The dependence of $\langle\Delta\mathcal{B}_d\rangle$ and $\Delta\mathcal{R}$ on the CKM parameters is worked out and the resulting constraints on the unitarity triangle from an eventual measurement of $\Delta\mathcal{R}$ are illustrated.

1 Introduction

With the advent of new and upgraded experimental facilities in the next year(s), flavour physics involving B decays will come under minute experimental and theoretical scrutiny. The overriding interest in these experiments is in measuring CP-violating asymmetries in partial B-decay rates, which will allow to quantitatively test the Kobayashi-Maskawa [1] paradigm of CP violation. In addition, the large number of B hadrons anticipated to be produced at these facilities (estimated to be $O(10^8)$ - $O(10^{12})$) will allow to measure a number of flavour-changing-neutral-current (FCNC) processes involving the transitions $b \to sX$ and $b \to dX$, with $X = \gamma, g, \ell^+\ell^-, \nu\bar{\nu}$, and B^0 - $\overline{B^0}$ mixings. In the context of the Standard Model (SM), FCNC decays and mixings measure the Cabibbo-Kobayashi-Maskawa (CKM) [1] matrix elements, in particular V_{td}, V_{ts} and V_{tb}. These quantities can, in principle, also be measured directly in top quark decays $t \to q_i W^+$, with $q_i = d, s, b$. A comparison of these matrix elements in the FCNC processes and direct measurements in t decays would provide one of the best strategies to search for new physics in B decays. So far, only V_{tb} has been directly measured at Fermilab, yielding $|V_{tb}| = 0.99 \pm 0.15$ [2].

Present knowledge of V_{td} owes itself to the measurements of ΔM_d, the mass difference in the B^0 - $\overline{B^0}$ complex. With the current world average $\Delta M_d = 0.471 \pm 0.016$ (ps)$^{-1}$, the error on V_{td} is dominated by theoretical uncertainty on the hadronic matrix element $f_{B_d}\sqrt{B_{B_d}}$, for which present Lattice-QCD estimates are $f_{B_d}\sqrt{B_{B_d}} = 215 \pm 35$ MeV [3], yielding $0.0065 \leq |V_{td}V_{tb}^*| \leq 0.010$. We also mention that a single event for the charged kaon decay mode $K^+ \to \pi^+\nu\bar{\nu}$ reported by the Brookhaven E787 experiment, yielding $\mathcal{B}(K^+ \to \pi^+\nu\bar{\nu}) = (4.2^{+9.7}_{-3.5}) \times 10^{-10}$, allows one to infer $0.006 \leq |V_{td}V_{tb}^*| \leq 0.06$ [4]. The branching ratio for the decay $B \to X_s\gamma$ has led to a determination of the matrix element V_{ts} [5], yielding $|V_{ts}V_{tb}^*| = 0.0035 \pm 0.004$, with the error dominated by the experimental error on the branching ratio $\mathcal{B}(B \to X_s + \gamma)$ [6,7]. These numbers can be taken as the measurements of $|V_{td}|$ and $|V_{ts}|$ by assuming the value $V_{tb} \simeq 1$ from the CKM unitarity, which holds to a very high accuracy [8].

In this paper, we pursue the idea of measuring the FCNC semileptonic decays $B \to X_s\ell^+\ell^-$ and $B \to X_d\ell^+\ell^-$, below the J/ψ- and above the ρ, ω-resonance regions in the dilepton invariant mass, to determine $|V_{ts}|$ and $|V_{td}|$, respectively, and the ratio $|V_{td}/V_{ts}|$ from the ratio of the branching ratios. In this context, these decays and the related ones, $B \to X_s\nu\bar{\nu}$ and $B \to X_d\nu\bar{\nu}$, were discussed some time ago [9]. The decays $B \to (X_s, X_d)\nu\bar{\nu}$ are practically free of long-distance complications [10] and the renormalization-scale dependence of the decay rates has also been brought under control [11]. Hence, these decays are theoretically remarkably clean but, unfortunately, they are difficult to measure in $\Upsilon(4S)$ decays and out of question in hadronic collisions. Using the

missing energy technique and LEP I data, the ALEPH collaboration has searched for the decays $B \to X_s \nu \bar{\nu}$ setting an upper bound $\mathcal{B}(B \to X_s \nu \bar{\nu}) < 7.7 \times 10^{-4}$ (at 90% C.L.) [12], which is a factor 20 away from the SM expectations [11]. While the discovery of these decays looks formidable elsewhere, a high luminosity Z^0-factory - being discussed in conjunction with an e^+e^- linear collider [13]- looks like having the best chance of measuring them. This possibility deserves a dedicated study.

The possibility of determining $|V_{td}/V_{ts}|$ from the ratio of the invariant mass decay distributions $\frac{dR}{ds} \equiv \frac{d\mathcal{B}}{ds}[B \to X_d \ell^+ \ell^-]/\frac{d\mathcal{B}}{ds}[B \to X_s \ell^+ \ell^-]$ away from the resonances was revisited by Kim, Morozumi and Sanda [14]. These authors included the effects of the leading order power corrections (in $1/m_b^2$) in the short-distance part of the dilepton invariant mass distribution and the long-distance contributions from the $c\bar{c}$-resonances, calculated in Ref. [15]. (For earlier-vintage derivations without the power corrections, see [16,17].) We reanalyze the decays $B \to X_s \ell^+ \ell^-$ and $B \to X_d \ell^+ \ell^-$ and the ratio of the branching ratios $\Delta\mathcal{R} \equiv \int ds \frac{d\mathcal{B}}{ds}[B \to X_d \ell^+ \ell^-]/\int ds \frac{d\mathcal{B}}{ds}[B \to X_s \ell^+ \ell^-]$, integrated over a kinematic range $q_{min}^2 \leq s \leq q_{max}^2$, designed to minimize the resonant contribution. Our theoretical treatment differs from that of Ref. [14] in a number of ways, summarized below.

- The dilepton invariant mass distributions in $B \to (X_s, X_d)\ell^+ \ell^-$ can be calculated in the context of the heavy quark effective theory (HQET) as a power expansion in regions far from the resonances, thresholds and end-points [15,10]. Away from the $J/\psi, \psi', ...$-resonances, the $1/m_c^2$-expansion provides, in principle, a viable description of the non-perturbative contributions arising from the $c\bar{c}$-loop [10]. The contribution of the light quark $q\bar{q}$-loops, which is not CKM-suppressed in the decay $B \to X_d \ell^+ \ell^-$, can likewise be calculated by doing an expansion of the decay amplitudes in Λ_{QCD}^2/q^2 in regions of the dilepton squared mass satisfying $q^2 \gg \Lambda_{QCD}^2$. Thus, the HQET framework provides an evaluation of the invariant dilepton mass spectrum in these processes with the present precision limited to the leading power corrections in $1/m_b^2$, $1/m_c^2$ and Λ_{QCD}^2/q^2. We present HQET-based calculations of the decay rates, CP asymmetries and the ratio $\Delta\mathcal{R}$.

- Away from the resonances and the end-points, the power corrections in $1/m_b^2$ calculated in HQET and in explicit wave function models, such as the Fermi motion (FM) model [18], yield very similar invariant dilepton mass [15] and hadron energy distributions [19] in the decays $B \to X_q \ell^+ \ell^-$. However, it is known that there are marked differences in estimates of the non-perturbative $c\bar{c}$-contribution, obtained by using the $1/m_c^2$-corrections in the HQET approach and alternative methods based on the Breit-Wigner-shaped resonant amplitudes [20,21]. Data may eventually pro-

3

vide a discrimination against some of these approaches, but currently at least four different variations on this theme exist in the literature [10,15,22,23]. This LD-uncertainty therefore compromises theoretical precision on decay rates and has to be taken into account. We calculate the theoretical uncertainties on the branching ratios for the decays $B \rightarrow (X_d, X_s)\ell^+\ell^-$, CP asymmetries and the ratio $\Delta\mathcal{R}$, showing numerically their impact on the determination of $|V_{ts}|$, $|V_{td}|$ and the CKM-Wolfenstein parameters ρ and η [24] from an eventual measurement of these decays.

- We reanalyze the renormalization scale dependence in the branching ratios for the decays $B \rightarrow X_s\ell^+\ell^-$ and $B \rightarrow X_d\ell^+\ell^-$, using the method employed by Kagan and Neubert in the radiative decay $B \rightarrow X_s + \gamma$ [25]. This approach avoids accidental cancellations among the individual scale-dependent contributions but gives a larger scale (μ)-dependence of the branching ratios than the method of evaluating the same in the total branching ratio [14]. The former is probably a more realistic estimate of the neglected higher order corrections.

We find that the partial branching ratio in the SM is uncertain by typically $\pm 13\%$ ($\pm 15\%$) for the decay $B \rightarrow X_s\ell^+\ell^-$ ($B \rightarrow X_d\ell^+\ell^-$), but the ratio $\Delta\mathcal{R}$ is remarkably stable with typical error less than several percent. Hence, $\Delta\mathcal{R}$ is well-suited to determine the ratio $|V_{td}/V_{ts}|$. However, the scale-dependence of the CP asymmetries in $B \rightarrow (X_s, X_d)\ell^+\ell^-$ is found to be huge, reflecting the (present) leading logarithmic theoretical accuracy of the CP-odd parts of the amplitudes. Without the power corrections and fixing the scale to $\mu = m_b$, the CP asymmetries in question have been studied earlier in Ref. [26]. We point out that these estimates are uncertain by almost $\pm 100\%$ due to the sensitive scale-dependence and their stabilization requires next-to-leading order corrections. In the case of the CP-even parts, we recall that the inclusion of the explicit $O(\alpha_s)$ corrections in the matrix elements has reduced the scale dependence of the decay rates considerably [27,28].

This paper is organized as follows: In section 2, we briefly review the derivation of the matrix elements and dilepton invariant mass distributions for the decays $B \rightarrow (X_s, X_d)\ell^+\ell^-$ including long-distance contributions in the four approaches: (i) AMM [17,15], (ii) KS [22], (iii) LSW [23] and (iv) HQET [10]. The partially integrated branching ratios and CP asymmetries are presented in section 3 where we also specify our input parameters. We show the scale dependence of the branching ratios $\Delta\mathcal{B}(\bar{B} \rightarrow \bar{X}_s\ell^+\ell^-)$ and $\Delta\mathcal{B}(\bar{B} \rightarrow \bar{X}_d\ell^+\ell^-)$ in the AMM approach and the contributions arising from the individual Wilson coefficients. We also present a comparative numerical study of the quantities $\langle\Delta\mathcal{B}_s\rangle$, $\langle\Delta\mathcal{B}_d\rangle$, $(a_{CP})_s$ and $(a_{CP})_d$ in the four mentioned approaches. Uncertainties arising from the other parameters (m_b, m_t and $\Lambda_{QCD}^{(5)}$) are worked out numer-

ically. With this we calculate the overall theoretical errors in these quantities and the ratio $\Delta \mathcal{R}$ and their impact on the determination of the CKM parameters. Finally, section 4 contains a brief comparison of the theoretical precision of $|V_{td}/V_{ts}|$ in the decays $B \to (X_s, X_d)\ell^+\ell^-$ with that of other methods proposed in the literature to determine the same ratio.

2 $B \to (X_d, X_s)\ell^+\ell^-$ Decays in the Effective Hamiltonian Approach

We work in the effective Hamiltonian approach, which is based on integrating out the heavy degrees of freedom $(t, W^\pm, Z^0)$, in the SM. The resulting effective Hamiltonian for the decays $B \to (X_d, X_s)\ell^+\ell^-$, $\mathcal{H}_{eff}(b \to q\ell^+\ell^-)$, can be expressed as follows:

$$
\begin{aligned}
\mathcal{H}_{eff}(b \to q\ell^+\ell^-) &= -\frac{4G_F}{\sqrt{2}} V_{tq}^* V_{tb} \sum_{i=1}^{10} C_i O_i \\
&+ \frac{4G_F}{\sqrt{2}} V_{uq}^* V_{ub} \left[C_1(O_1^{(u)} - O_1) + C_2(O_2^{(u)} - O_2) \right] ,
\end{aligned}
\tag{1}
$$

where V_{ij} are the CKM matrix elements. The C_i are the Wilson coefficients, which depend, in general, on the renormalization scale μ, except for C_{10}, and can be seen in leading logarithmic approximation in [27]. The operators are defined as follows:

$$
\begin{aligned}
O_1 &= (\bar{q}_{L\alpha} \gamma_\mu b_{L\alpha})(\bar{c}_{L\beta} \gamma^\mu c_{L\beta}) , \\
O_2 &= (\bar{q}_{L\alpha} \gamma_\mu b_{L\beta})(\bar{c}_{L\beta} \gamma^\mu c_{L\alpha}) , \\
O_3 &= (\bar{q}_{L\alpha} \gamma_\mu b_{L\alpha}) \sum_{q'=u,d,s,c,b} (\bar{q}'_{L\beta} \gamma^\mu q'_{L\beta}) , \\
O_4 &= (\bar{q}_{L\alpha} \gamma_\mu b_{L\beta}) \sum_{q'=u,d,s,c,b} (\bar{q}'_{L\beta} \gamma^\mu q'_{L\alpha}) , \\
O_5 &= (\bar{q}_{L\alpha} \gamma_\mu b_{L\alpha}) \sum_{q'=u,d,s,c,b} (\bar{q}'_{R\beta} \gamma^\mu q'_{R\beta}) , \\
O_6 &= (\bar{q}_{L\alpha} \gamma_\mu b_{L\beta}) \sum_{q'=u,d,s,c,b} (\bar{q}'_{R\beta} \gamma^\mu q'_{R\alpha}) , \\
O_7 &= \frac{e}{16\pi^2} \bar{q}_\alpha \sigma_{\mu\nu} (m_b R + m_q L) b_\alpha F^{\mu\nu} , \\
O_8 &= \frac{g}{16\pi^2} \bar{q}_\alpha T_{\alpha\beta}^a \sigma_{\mu\nu} (m_b R + m_q L) b_\beta G^{a\mu\nu}, \\
O_9 &= \frac{e^2}{16\pi^2} \bar{q}_\alpha \gamma^\mu L b_\alpha \bar{\ell} \gamma_\mu \ell , \\
O_{10} &= \frac{e^2}{16\pi^2} \bar{q}_\alpha \gamma^\mu L b_\alpha \bar{\ell} \gamma_\mu \gamma_5 \ell ,
\end{aligned}
\tag{2}
$$

where L and R denote chiral projections, $L(R) = 1/2(1 \mp \gamma_5)$. Here, unitarity of the CKM matrix has been used in writing the flavour structure of a generic FCNC $b \to q$

transition amplitude $\mathcal{T}^{(q)}$ in the form

$$\mathcal{T}^{(q)} = \sum_{i=u,c,t} \lambda_i^{(q)} \mathcal{T}_i = \lambda_t^{(q)}(\mathcal{T}_t - \mathcal{T}_c) + \lambda_u^{(q)}(\mathcal{T}_u - \mathcal{T}_c) , \tag{3}$$

where $\lambda_i^{(q)} = V_{iq}^* V_{ib}$ and $q = d, s$. For the $b \to s$ transitions, the second term in Eq. (3) can be safely neglected as $\lambda_u^{(s)} \ll \lambda_t^{(s)}$. However, for the $b \to d$ transitions, the CKM factors $\lambda_u^{(d)}$ and $\lambda_t^{(d)}$ are of the same order and hence all terms in Eq. (3) must be kept. The operator basis given in Eq. (1) has been written in accordance with Eq. (3) and includes the Four-Fermi operators containing a $u\bar{u}$ pair,

$$\begin{aligned}
O_1^{(u)} &= (\bar{q}_{L\alpha}\gamma_\mu b_{L\alpha})(\bar{u}_{L\beta}\gamma^\mu u_{L\beta}) , \\
O_2^{(u)} &= (\bar{q}_{L\alpha}\gamma_\mu b_{L\beta})(\bar{u}_{L\beta}\gamma^\mu u_{L\alpha}) .
\end{aligned} \tag{4}$$

The matrix element for the decays $b \to q\ell^+\ell^-$ $(q = d, s)$ can be written as

$$\begin{aligned}
\mathcal{M}(b \to q\ell^+\ell^-) &= \frac{G_F \alpha}{\sqrt{2}\pi} V_{tq}^* V_{tb} \left[\left(C_{9q}^{\text{eff}} - C_{10} \right) (\bar{q}\,\gamma_\mu\, L\, b) \left(\bar{\ell}\,\gamma^\mu\, L\, \ell \right) \right. \\
&+ \left(C_{9q}^{\text{eff}} + C_{10} \right) (\bar{q}\,\gamma_\mu\, L\, b) \left(\bar{\ell}\,\gamma^\mu\, R\, \ell \right) \\
&- \left. 2 C_7^{\text{eff}} \left(\bar{q}\, i\,\sigma_{\mu\nu}\, \frac{q^\nu}{q^2}(m_q L + m_b R)\, b \right) \left(\bar{\ell}\,\gamma^\mu\, \ell \right) \right] .
\end{aligned} \tag{5}$$

Here $q^\nu \equiv p_+^\nu + p_-^\nu$ denotes the Four-momentum of the invariant dilepton system, where $p_\pm$ are the corresponding momenta of the $\ell^\pm$; $s \equiv q^2$ is the invariant dilepton mass squared. The effective coefficients of O_9 are given by

$$C_{9q}^{\text{eff}}(\hat{s}) = C_9 \eta(\hat{s}) + Y^q(\hat{s}) . \tag{6}$$

The functions $\eta(\hat{s})$ and $Y^q(\hat{s})$ represent the $\mathcal{O}(\alpha_s)$ correction [29] and the (perturbative) one loop matrix element of the Four-Fermi operators [27,28], respectively. We have in the (naive dimensional regularization) NDR-scheme, which we use throughout our work,

$$\begin{aligned}
Y^q(\hat{s}) &= g(\hat{m}_c, \hat{s})\,(3\,C_1 + C_2 + 3\,C_3 + C_4 + 3\,C_5 + C_6) \\
&- \frac{1}{2}g(1, \hat{s})\,(4\,C_3 + 4\,C_4 + 3\,C_5 + C_6) - \frac{1}{2}g(0, \hat{s})\,(C_3 + 3\,C_4) \\
&+ \frac{2}{9}\,(3\,C_3 + C_4 + 3\,C_5 + C_6) - \frac{V_{uq}^* V_{ub}}{V_{tq}^* V_{tb}}(3C_1 + C_2)(g(0, \hat{s}) - g(\hat{m}_c, \hat{s})) ,
\end{aligned} \tag{7}$$

where we have introduced the dimensionless variable $\hat{s} \equiv q^2/m_b^2$ and $\hat{m}_c \equiv m_c/m_b$. The functions $\eta(\hat{s})$ and $g(z, \hat{s})$ can be seen elsewhere [27,20]. Note that the renormalization scheme-dependence of the function $Y^q(\hat{s})$ cancels with the corresponding one in C_9. The effective coefficient of the $bs\gamma$ vertex is given by $C_7^{\text{eff}} = C_7 - C_5/3 - C_6$ [30].

The dilepton invariant mass spectrum including power corrections in the HQET approach in $B \to X_q \ell^+ \ell^-$ decays can be written as:

$$\frac{d\mathcal{B}}{d\hat{s}} = \frac{d\mathcal{B}^0}{d\hat{s}} + \frac{d\mathcal{B}^{1/m_b^2}}{d\hat{s}} + \frac{d\mathcal{B}^{1/q^2}}{d\hat{s}} \ , \tag{8}$$

where the first term corresponds to the parton model [27,28], the second term accounts for the $\mathcal{O}(1/m_b^2)$ power corrections [15], and the last term accounts for the non-perturbative interaction of a virtual $u\bar{u}$- and $c\bar{c}$-quark loop with soft gluons. The explicit expression for $d\mathcal{B}^{1/q^2}/d\hat{s}$ for $m_q = 0$ can be deduced from the literature [10]

$$\frac{d\mathcal{B}^{1/q^2}}{d\hat{s}} = -\mathcal{B}_0 C_2 \lambda_2 \frac{32}{27}(1-\hat{s})^2 \tag{9}$$

$$\times Re \left\{ \left[C_7^{\text{eff}*} \frac{(1+6\hat{s}-\hat{s}^2)}{\hat{s}} + C_{9q}^{\text{eff}(0)*}(\hat{s})(2+\hat{s}) \right] \left[\frac{F(s,m_c)}{m_c^2} - \frac{\lambda_u^{(q)}}{\lambda_t^{(q)}} \left(\frac{F(s,m_u)}{m_u^2} - \frac{F(s,m_c)}{m_c^2} \right) \right] \right.$$

$$\left. + [(3C_1 + C_2)(g(0,\hat{s}) - g(\hat{m}_c,\hat{s}))]^* (2+\hat{s}) \left[|\frac{\lambda_u^{(q)}}{\lambda_t^{(q)}}|^2 \left(\frac{F(s,m_u)}{m_u^2} - \frac{F(s,m_c)}{m_c^2} \right) - \frac{\lambda_u^{(q)}}{\lambda_t^{(q)}} \frac{F(s,m_c)}{m_c^2} \right] \right\}.$$

The branching ratio for $B \to X_q \ell^+ \ell^-$ is expressed in terms of the measured semileptonic branching ratio $\mathcal{B}_{sl}$ for the decays $B \to X_c \ell \nu_\ell$. This fixes the normalization

$$\mathcal{B}_0 \equiv \mathcal{B}_{sl} \frac{3\,\alpha^2}{16\pi^2} \frac{|V_{tq}^* V_{tb}|^2}{|V_{cb}|^2} \frac{1}{f(\hat{m}_c)\kappa(\hat{m}_c)} \ , \tag{10}$$

where $f(\hat{m}_c), \kappa(\hat{m}_c)$ can be seen, for example, in [15]. The function $F(s,m) \equiv F(r)$ with $r = s/(4m^2)$ is given in [10]. In the region $r \gg 1$, $F(s,m_u)/m_u^2 \propto 1/s$. The condition $r \gg 1$ is well satisfied, for example, for $q^2 \geq 1.0$ GeV^2 (for which $r > 25$). In this region, the operator product expansion (OPE) is not in '$1/m_u^2$' but in Λ_{QCD}^2/q^2. Hence, there is a sufficiently large region in q^2 where the OPE holds in $1/m_b^2$, $1/m_c^2$ and Λ_{QCD}^2/q^2. Note also that for the terms proportional to the power corrections, we use $C_{9q}^{\text{eff}(0)*}(\hat{s})$ which equals $C_{9q}^{\text{eff}*}(\hat{s})$ with $\eta(\hat{s}) = 1$.

In $B \to X_q \ell^+ \ell^-$ decays $c\bar{c}$-resonances are present via $B \to X_q + (J/\psi, \psi', ...) \to X_q \ell^+ \ell^-$. Their implementation and the corresponding uncertainties in the $B \to X_s \ell^+ \ell^-$ case have been discussed recently by us [20]. There are at least four different Ansätze advocated in the literature in this context, summarized below.

- The HQET-based approach [10], where the non-perturbative $c\bar{c}$-contribution away from the $(J/\psi, \psi', ...)$-resonances is implemented by the $1/m_c^2$ terms in the expression for $d\mathcal{B}^{1/q^2}/d\hat{s}$.

- One could add the resonant $c\bar{c}$-contribution, parametrized using a Breit-Wigner shape with the normalizations fixed by data, to the complete perturbative contribution resulting from the $c\bar{c}$-loop. This scheme has been used in a number of papers [17,15,14,20].

The effective coefficients including the $c\bar{c}$-resonances are defined as

$$C_{9q}^{\text{eff}}(\hat{s}) \equiv C_9 \eta(\hat{s}) + Y^q(\hat{s}) + Y_{res}{}^q(\hat{s}) , \tag{11}$$

where $Y^q(\hat{s})$ has been given earlier and $Y_{res}{}^q(\hat{s})$ in this scheme is defined as:

$$
\begin{aligned}
Y_{res}{}^q(\hat{s}) &= \frac{3\pi}{\alpha^2}\kappa \left(-\frac{V_{cq}^* V_{cb}}{V_{tq}^* V_{tb}} C^{(0)} - \frac{V_{uq}^* V_{ub}}{V_{tq}^* V_{tb}}(3\,C_3 + C_4 + 3\,C_5 + C_6) \right) \\
&\times \sum_{V_i=\psi(1s),\ldots,\psi(6s)} \frac{\Gamma(V_i \to \ell^+\ell^-)\,M_{V_i}}{M_{V_i}{}^2 - \hat{s}\,m_b{}^2 - iM_{V_i}\Gamma_{V_i}} ,
\end{aligned}
\tag{12}
$$

with $C^{(0)} \equiv 3C_1 + C_2 + 3C_3 + C_4 + 3C_5 + C_6$. In what follows we shall neglect the part $\sim \frac{V_{uq}^* V_{ub}}{V_{tq}^* V_{tb}}$ in Eq. (12) in our numerical analysis, since the particular combination of the Wilson coefficients appearing in this term is strongly suppressed compared to $C^{(0)}$. Further, since data only determines the product $\kappa C^{(0)} = 0.875$ [8], we keep this fixed. For ease of writing, we call this approach the AMM approach [17].

The remaining two approaches are the following:

- The LSW-approach [23]: Here, for the non-resonant $c\bar{c}$-contribution, only the constant term in $g(\hat{m}_c, \hat{s})$ is kept. Calling it $\tilde{g}(\hat{m}_c, \hat{s})$, it is given by $\tilde{g}(\hat{m}_c, \hat{s}) = -\frac{8}{9}\ln(m_b/\mu) - \frac{8}{9}\ln \hat{m}_c + \frac{8}{27}$. The resonant $c\bar{c}$ part is essentially as given in Eq. (12).

- The KS-approach [22], in which the function $C_{9q}^{\text{eff}}(\hat{s})$ is parametrized using a dispersion approach. For details and further discussions of this approach, we refer to [22,20].

In $B \to X_d \ell^+\ell^-$ decays, in addition to the $c\bar{c}$ bound states, also the $u\bar{u}$ bound states have to be included in the decay amplitudes. We have calculated the dilepton invariant mass distribution, using the Breit-Wigner shape for the resonances, as discussed earlier, and taking the widths and partial leptonic widths from the Particle Data Group [8]. However, numerically the $u\bar{u}$-resonant part is less important, as the leptonic branching ratios $\mathcal{B}(V^0 \to e^+e^-)$ and $\mathcal{B}(V^0 \to \mu^+\mu^-)$ for the dominant resonances $V^0 = \rho^0, \omega$ are small [8]. Moreover, their effect is reduced by imposing a cut on the dilepton invariant mass, say $q^2 > 1\text{GeV}^2$, which we have explicitly checked. Higher states like ρ', ω' have larger

8

widths and are thus expected to play minor roles due to their smaller branching ratios in dilepton pairs.

In the three approaches discussed above (AMM,LSW,KS) we include the $1/m_b^2$-corrections, calculated in the phenomenological Fermi motion model (FM) [18], which implements such effects in terms of the B-meson wave function effects. The implementation of the FM model in $B \to X_s \ell^+ \ell^-$ decays in the dilepton invariant mass distribution can be seen in [15], which we also adopt here for the calculations of the distributions in $B \to X_d \ell^+ \ell^-$. We note that the branching ratios in the HQET-based $1/m_b^2$ approach and the FM-model are very close to each other for identical values of the input parameters.

3   Branching Ratios and CP Asymmetries in $B \to X_q \ell^+ \ell^-$

3.1   Numerical input and definitions of the partial branching ratios and CP asymmetries

We now specify how we determine theoretical uncertainties in the branching ratios, the ratio $\Delta \mathcal{R}$, and CP asymmetries in the decays $B \to (X_s, X_d) \ell^+ \ell^-$. The dispersion in

Table 1: Default values of the input parameters and the $\pm 1\ \sigma$ errors on the sensitive parameters used in our numerical calculations.

m_W	80.41 GeV
m_Z	91.1867 GeV
$\sin^2 \theta_W$	0.2255
m_s	0.2 GeV
m_d	0.01 GeV
m_b	4.8 ± 0.2 GeV
m_t	173.8 ± 5.0 GeV
μ	$m_b{}^{+m_b}_{-m_b/2}$
$\Lambda_{QCD}^{(5)}$	$0.220^{+0.078}_{-0.063}$ GeV
α^{-1}	129
$\alpha_s(m_Z)$	0.119 ± 0.0058
$\mathcal{B}_{sl}$	(10.4 ± 0.4) %

the values of the obsevables due to the errors in the input parameters $m_b, \mu, m_t, \alpha_s(m_Z)$ (equivalently $\Lambda_{QCD}^{(5)}$), and $\mathcal{B}_{sl}$, given in Table 1, is calculated by varying one parameter at a time. To estimate the uncertainty from the b-quark mass in the FM model, we explore the parameter space of this model with three sets of parameters: $(p_F, m_q) = (520, 280), (450, 0), (245, 0)$ in (MeV,MeV), which correspond to an effective b-quark

mass of $m_b^{\text{eff}} = 4.6, 4.8, 5.0$ GeV, respectively. We set $m_c = m_b^{\text{eff}}(m_b) - 3.4$ GeV in both the FM-model and HQET analysis. Comparison with the HQET prediction [15] is worked out for $\lambda_1 = -0.20$ GeV^2 and $\lambda_2 = 0.12$ GeV^2, as the dependence of the branching ratios on these parameters is small. The individual errors are then added in quadrature to get the final cumulative error.

We proceed by defining the partly integrated branching ratios ($q = s, d$):

$$\Delta \mathcal{B}_q \equiv \int_{q_{\min}^2}^{q_{\max}^2} dq^2 \frac{d\mathcal{B}(B \to X_q \ell^+ \ell^-)}{dq^2} ,\tag{13}$$

together with $\Delta \bar{\mathcal{B}}_q$, for the CP-conjugate decays $\bar{B} \to \bar{X}_q \ell^+ \ell^-$, and the branching ratio averaged over the charge-conjugated states:

$$\langle \Delta \mathcal{B}_q \rangle \equiv \frac{\Delta \mathcal{B}_q + \Delta \bar{\mathcal{B}}_q}{2} ,\tag{14}$$

The CP asymmetry in the partial rates for $B \to X_q \ell^+ \ell^-$ is defined as:

$$(a_{CP})_q \equiv \frac{\Delta \mathcal{B}_q - \Delta \bar{\mathcal{B}}_q}{\Delta \mathcal{B}_q + \Delta \bar{\mathcal{B}}_q} .\tag{15}$$

We further decompose the partial branching ratios $\Delta \mathcal{B}_q$ in terms of the CKM factors

$$\Delta \mathcal{B}_q = (|\lambda_t^{(q)}|^2 D_t^{(q)} + |\lambda_u^{(q)}|^2 D_u^{(q)} + Re(\lambda_t^{(q)*} \lambda_u^{(q)}) D_r^{(q)} + Im(\lambda_t^{(q)*} \lambda_u^{(q)}) D_i^{(q)})/|V_{cb}|^2 ,\tag{16}$$

from which the CP conjugated branching ratio $\Delta \bar{\mathcal{B}}_q$ can be obtained by substituting $\lambda_{u,t}^{(q)} \to \lambda_{u,t}^{(q)*}$. Hence, the charge-conjugate averaged branching ratio $\langle \Delta \mathcal{B}_q \rangle$ is obtained from $\Delta \mathcal{B}_q$ by dropping the $Im(\lambda_t^{(q)*} \lambda_u^{(q)})$ term. The CP asymmetry is given by the expression:

$$(a_{CP})_q = Im(\lambda_t^{(q)*} \lambda_u^{(q)}) D_i^{(q)}/(|V_{cb}|^2 \langle \Delta \mathcal{B}_q \rangle) .\tag{17}$$

The functions $D_j^{(q)}$, $j = t, u, r, i$ depend on the input parameters, which we have specified in Table 1, and on the interval in q^2, specified by q_{min}^2 and q_{max}^2. We shall work always above the (ρ, ω)- and below the J/ψ-resonances in the so-called low-q^2 region with q_{min}^2 and q_{max}^2 taken as

$$q_{\min}^2 = 1.0 \text{ GeV}^2 \leq q^2 \leq 6.0 \text{ GeV}^2 = q_{\max}^2 .\tag{18}$$

We use the Wolfenstein representation of the CKM matrix [24] with $A = 0.819$ and $\lambda = 0.2196$ fixed, as the errors on these quantities are small [8]. The other two
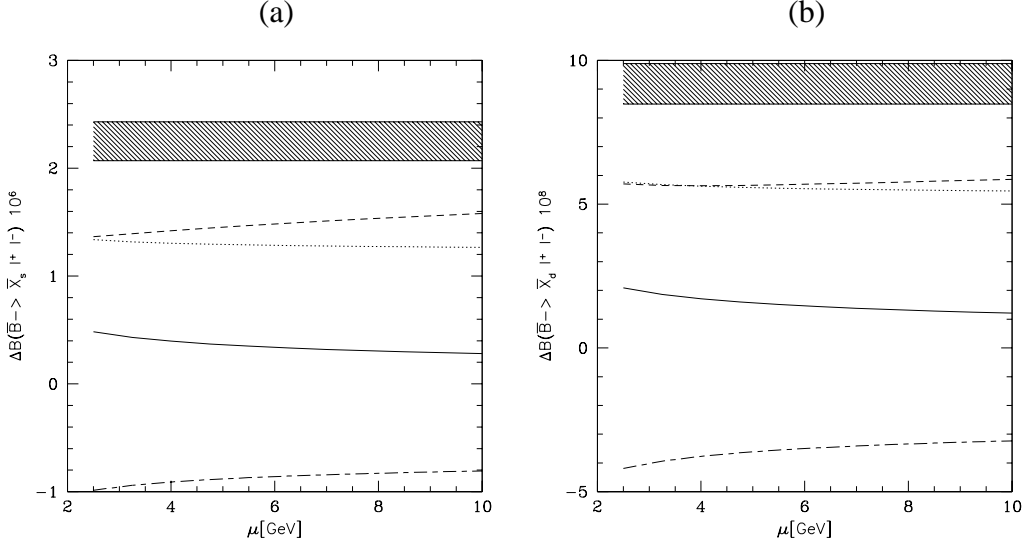
Figure 1: Renormalization scale (μ)-dependence of the individual terms and the partly integrated branching ratios ΔB_s for the decay $\bar{B} \to \bar{X}_s \ell^+ \ell^-$ (a) and ΔB_d for $\bar{B} \to \bar{X}_d \ell^+ \ell^-$ (b), calculated in the AMM-approach. The solid, dotted, dashed, long-short dashed curves correspond to the contributions proportional to the effective Wilson coefficients $|C_7^{\text{eff}}|^2$, $|C_{10}|^2$, $|C_9^{\text{eff}}|^2$ and $Re(C_7^{\text{eff}} C_9^{\text{eff}})$, respectively. The resulting μ uncertainty in the branching ratio, obtained by adding the weighted errors in quadrature, is indicated by the shaded area.

parameters (ρ, η) are implicitly the subject of the present work. Defining $\bar{\rho} = \rho(1 - \frac{\lambda^2}{2})$ and $\bar{\eta} = \eta(1 - \frac{\lambda^2}{2})$, we have up to terms of order λ^6 [31]:

$$\lambda_u^{(s)} = A\lambda^4(\rho - i\eta) , \qquad \lambda_t^{(s)} = -A\lambda^2 \left[1 - \frac{\lambda^2}{2} + \lambda^2(\rho - i\eta) \right] , \qquad (19)$$

$$\lambda_u^{(d)} = A\lambda^3(\bar{\rho} - i\bar{\eta}) , \qquad \lambda_t^{(d)} = A\lambda^3(1 - \bar{\rho} + i\bar{\eta}) , \qquad (20)$$

and $V_{cb} = A\lambda^2$. It follows that $\left| \frac{V_{td}}{V_{ts}} \right|^2 = \lambda^2(1 + \lambda^2(1 - 2\bar{\rho}))((1 - \bar{\rho})^2 + \bar{\eta}^2) + O(\lambda^6)$. Global fits of the CKM parameters have been performed in a number of papers [32–34], with very similar (though not identical) results. For illustration, we shall use the results of the CKM fits from Ref. [32], yielding:

$$\rho = 0.155^{+0.115}_{-0.105} , \qquad \eta = 0.383^{+0.063}_{-0.060} . \qquad (21)$$

3.2 Parametric dependence of the branching ratios and CP asymmetries

We study the scale (μ)-dependence of the branching ratios along the lines followed in [25] in the $B \to X_s\gamma$ case. Thus, instead of varying the scale μ between $m_b/2$ and

$2m_b$ in the full expression for the respective branching ratios (the naive method), the scale-dependence of the individual terms involving different Wilson coefficient combinations is calculated independently and the resulting errors are added in quadrature. It is a conservative approach and avoids the possibility of accidental cancellations of the scale-dependence in the various terms, which takes place in the SM in both the $B \to X_s \gamma$ case [25] and in $B \to X_q \ell^+ \ell^-$, as shown here. For the branching ratio in $B \to X_q \ell^+ \ell^-$ decays the relevant coefficients are: $|C_{10}|^2, |C_9^{\text{eff}}|^2, Re(C_7^{\text{eff}} C_9^{\text{eff}})$ and $|C_7^{\text{eff}}|^2$. Of these, C_{10} does not renormalize, however, there is a residual dependence on μ from the normalization for which inclusive semileptonic branching ratio is used, bringing in an extra $\alpha_s(\mu)$-dependence.

The scale-dependence of the individual contributions from the specified Wilson coefficients to the branching ratios $\Delta \bar{\mathcal{B}}_s$ and $\Delta \bar{\mathcal{B}}_d$ and the branching ratios themselves, are shown in Fig. 1(a) and 1(b), respectively. We find for the scale dependence of $\Delta \bar{\mathcal{B}}_s$ an uncertainty $(+9.0, -7.3)\%$, measured from the reference value $\mu = m_b$. This is to be compared with the corresponding uncertainties $(+4.1, -1.3)\%$ calculated in the naive approach. The estimated μ-dependent uncertainty in $\Delta \bar{\mathcal{B}}_d$ is found to be $(+7.7, -7.6)\%$, compared to 2% in the naive approach.

Table 2: Values of the charge-conjugate averaged partial branching ratios $\langle \Delta \mathcal{B}_s \rangle$ and $\langle \Delta \mathcal{B}_d \rangle$ and the CP asymmetries $(a_{CP})_s$ and $(a_{CP})_d$, in the four LD-approaches AMM [17], KS [22], LSW [23] and HQET [10], discussed in the text. In the top part of the table (above the horizontal line), the parameters are fixed to their central values given in Table 1 and Eq. (21). In the lower part of the table, the parametric dependence of the observables on m_b, m_t and $\Lambda_{QCD}^{(5)}$, calculated using the AMM-approach, is listed.

	$\langle \Delta \mathcal{B}_s \rangle [10^{-6}]$	$(a_{CP})_s [\%]$	$\langle \Delta \mathcal{B}_d \rangle [10^{-8}]$	$(a_{CP})_d [\%]$
AMM	2.22	-0.19	9.61	4.40
KS	2.05	-0.18	8.83	4.09
LSW	2.31	-0.19	9.98	4.51
HQET	2.06	-0.17	8.93	4.02
$m_b = 4.6\text{GeV}$	2.15	-0.19	9.29	4.48
$m_b = 5.0\text{GeV}$	2.32	-0.18	10.03	4.29
$m_t = 178.2\text{GeV}$	2.36	-0.18	10.18	4.18
$m_t = 168.2\text{GeV}$	2.10	-0.20	9.06	4.63
$\Lambda_{QCD}^{(5)} = 0.298\text{GeV}$	2.20	-0.16	9.52	3.74
$\Lambda_{QCD}^{(5)} = 0.157\text{GeV}$	2.24	-0.22	9.70	5.03

The dependence of the charge-conjugate averaged branching ratios $\langle \Delta \mathcal{B}_s \rangle$ and $\langle \Delta \mathcal{B}_d \rangle$,

12

and the CP asymmetries $(a_{CP})_s$ and $(a_{CP})_d$ on the four schemes concerning the $c\bar{c}$-contribution is shown in the upper part of Table 2. For all these entries, we have fixed the parameters to their central values given in Table 1 and Eq. (21). The dependence of these observables on m_b, m_t and $\Lambda_{QCD}^{(5)}$, obtained in the AMM-scheme by varying only one parameter at a time, is shown in the lower part of Table 2. For the central values of ρ and η, the partial branching ratios are found to vary in the four approaches in the range: $2.05 \times 10^{-6} \leq \langle \Delta \mathcal{B}_s \rangle \leq 2.31 \times 10^{-6}$ and $8.83 \times 10^{-8} \leq \langle \Delta \mathcal{B}_d \rangle \leq 9.98 \times 10^{-8}$. For the same values of ρ and η but taking into account in addition the rest of the parametric uncertainties in Table 2, $\mathcal{B}_{sl}$, and the scale-dependence from Fig. 1(a) and 1(b), we find:

$$
\begin{aligned}
\langle \Delta \mathcal{B}_s \rangle &= \left(2.22^{+0.29}_{-0.30}\right) \times 10^{-6} , \\
\langle \Delta \mathcal{B}_d \rangle &= \left(9.61^{+1.32}_{-1.47}\right) \times 10^{-8} .
\end{aligned}
\tag{22}
$$

Thus, apart from the CKM-parametric dependence, we estimate $\pm 13\%$ uncertainty on $\langle \Delta \mathcal{B}_s \rangle$ and somewhat larger, $\pm 15\%$, on $\langle \Delta \mathcal{B}_d \rangle$. These errors are significantly larger than what one comes across in the literature. The present experimental bound is $\mathcal{B}(B \to X_s \ell^+ \ell^-) < 4.2 \times 10^{-5}$ (at 90% C.L.) [35]. We are not aware of a corresponding bound on $\mathcal{B}(B \to X_d \ell^+ \ell^-)$.

The branching ratio $\langle \Delta \mathcal{B}_d \rangle$, calculated in HQET, is shown in Fig. 2 as a function of the CKM parameter ρ for three fixed values of η, which correspond to the central value and the 95% C.L. bounds given in Eq. (21). The other input parameters have been fixed to their central values given in Table 1. In the allowed CKM parameter space, this partial branching ratio varies by a factor 3. As the theoretical error from the rest of the parameters is estimated to be $\pm 15\%$, the measurement of $\langle \Delta \mathcal{B}_d \rangle$ should allow to determine ρ and η. The ratio $\Delta \mathcal{R} = \langle \Delta \mathcal{B}_d \rangle / \langle \Delta \mathcal{B}_s \rangle$ has lot less theoretical error, as shown below.

The CP asymmetry, $(a_{CP})_s$ defined in eq. (15) in the $b \to s$ case in the SM is small. Hence its measurement can be used to search for new sources of CP violation in the $b \to s \ell^+ \ell^-$ transition. Numerically, the CP asymmetries are more uncertain reflecting in particular the scale-dependence of the functions $D_i^{(q)}$. A qualitatively similar behaviour has also been noted for the CP asymmetries in the radiative decays $B \to X_s + \gamma$ and $B \to X_d + \gamma$ in [37]. However, the scale-dependence of the CP asymmetries is more marked in the decays $B \to (X_s, X_d) \ell^+ \ell^-$ due to cancellations in two different products of the Wilson coefficients entering in $D_i^{(q)}$. (Specifically, between $C_7^{\text{eff}} Im(C_{9q}^{\text{eff}}|_u)$ and $Im(C_{9q}^{\text{eff}}|_u C_{9q}^{\text{eff}*}|_t)$, with $C_{9q}^{\text{eff}}|_x$ denoting the part in C_{9q}^{eff} which is proportional to the CKM factor $\lambda_x^{(q)}$.) This can be seen in Fig. 3, where we show the μ-dependence of the two mentioned contributions in $D_i^{(d)}$, and the function $D_i^{(d)}$ itself calculated in the naive and independent approaches. The function $D_i^{(s)}$ is very similar and hence not shown. The μ-dependence of $D_i^{(d)}$ in the naive approach, shown by the long-short dashed curve, is

13

very marked and it gets further accentuated in the independent approach, shown by the two dashed curves. For the central values of the CKM parameters and estimating the μ-dependence in the independent approach, we find:

$$
\begin{aligned}
(a_{CP})_s &= -(0.19^{+0.17}_{-0.19})\% \,, \\
(a_{CP})_d &= (4.40^{+3.87}_{-4.46})\%.
\end{aligned}
\tag{23}
$$

The corresponding numbers in the naive scale-dependent method are: $(a_{CP})_s = -(0.19^{+0.12}_{-0.13})\%$, and $(a_{CP})_d = (4.40^{+2.77}_{-3.23})\%$. In either case, Fig. 3 underscores the importance of calculating the next-to-leading order effects in $(a_{CP})_q$.
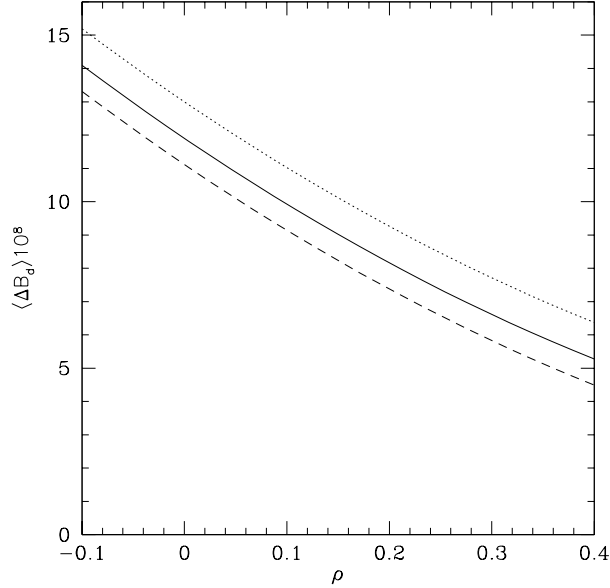
Figure 2: The charge-conjugate averaged partial branching ratio $\langle \Delta \mathcal{B}_d \rangle$ in the HQET-approach for the decay $B \to X_d \ell^+ \ell^-$ as a function of the CKM parameter ρ for three values of η; solid curve ($\eta = 0.383$), dotted curve ($\eta = 0.5$), dashed curve ($\eta = 0.27$).

3.3   Extraction of $\left| \frac{V_{td}}{V_{ts}} \right|$

For a precise determination of $\frac{|V_{td}|}{|V_{ts}|}$ (equivalently the CKM parameters), we calculate the ratio:

$$
\Delta \mathcal{R} \equiv \frac{\langle \Delta \mathcal{B}_d \rangle}{\langle \Delta \mathcal{B}_s \rangle} \,.
\tag{24}
$$

In terms of the CKM parameters and the functions $D_t^{(s)}$ and $D_j^{(d)}$ with $j = t, u, r$, defined earlier:

$$
\Delta \mathcal{R} = \lambda^2 \frac{(1 - \bar{\rho})^2 + \bar{\eta}^2) D_t^{(d)} + (\bar{\rho}^2 + \bar{\eta}^2) D_u^{(d)} + (\bar{\rho}(1 - \bar{\rho}) - \bar{\eta}^2) D_r^{(d)}}{(1 - \lambda^2(1 - 2\rho)) D_t^{(s)}} \,,
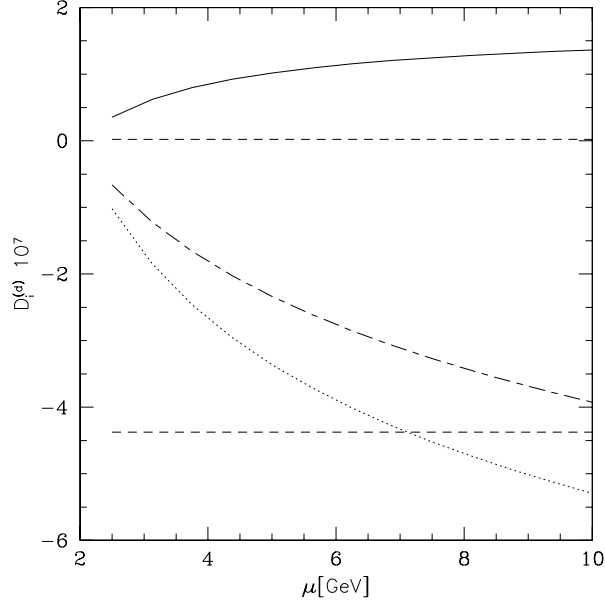\tag{25}
$$

14

Figure 3: Renormalization scale (μ)-dependence of the individual contributions and the function $D_i^{(d)}$, calculated in the AMM-approach. The solid and dotted curves correspond to the contributions proportional to the effective Wilson coefficients $C_7^{\text{eff}} Im(C_9^{\text{eff}}|_u)$ and $Im(C_9^{\text{eff}}|_u C_9^{\text{eff}*}|_t)$, respectively. The naive μ dependence is shown by the long-short dashed curve. The resulting μ uncertainty in the independent approach is bounded by the dashed lines.

where we have neglected terms proportional to $\lambda_u^{(s)}/\lambda_t^{(s)}$. A simpler form for $\Delta\mathcal{R}$ follows, if one notes that the functions $D_t^{(d)}$ and $D_t^{(s)}$ are equal for all practical purposes (see Table 3). Hence, setting $D_t^{(d)} = D_t^{(s)}$, one has

$$\Delta\mathcal{R} = \lambda^2 \frac{(1-\bar{\rho})^2 + \bar{\eta}^2)}{(1-\lambda^2(1-2\rho))} \left[1 + \frac{(\bar{\rho}^2 + \bar{\eta}^2)}{(1-\bar{\rho})^2 + \bar{\eta}^2)} \frac{D_u^{(d)}}{D_t^{(s)}} + \frac{(\bar{\rho}(1-\bar{\rho}) - \bar{\eta}^2)}{(1-\bar{\rho})^2 + \bar{\eta}^2)} \frac{D_r^{(d)}}{D_t^{(s)}} \right] . \quad (26)$$

The overall CKM factor is just the ratio $|V_{td}|^2/|V_{ts}|^2$. Note that the first (and dominant) term is independent of the dynamical details. The ratio $D_u^{(d)}/D_t^{(s)}$ is found to be numerically small (but model dependent, varying between 1.03×10^{-2} for the KS-approach and 2.16×10^{-2} for the LSW approach). The ratio $D_r^{(d)}/D_t^{(s)}$ is, in general, larger and it depends more sensitively on the estimate of the long-distance $c\bar{c}$-contribution, varying between $+0.14$ (for the LSW-approach) and -0.12 (in HQET). However, the multiplicative CKM factor accompanying this term in Eq. (26) being small comes to rescue. For example, for $\bar{\rho} = 0.151$ and $\bar{\eta} = 0.374$, this factor is only -0.012. Hence, for these values, we find $\Delta\mathcal{R} = (4.32 \pm 0.03)\%$. For other values of the CKM parameters, the uncertainty is larger and we quantify it later. The ratio $\Delta\mathcal{R}$ as a function of ρ is shown in Fig. 4 for the HQET-method. The three curves correspond to $\eta = 0.5$ (dotted curve), $\eta = 0.383$ (solid

curve), and $\eta = 0.27$ (dashed curve).

Table 3: Values of the functions $D_j^{(d)}$, $j = u, t, r, i$ and $D_t^{(s)}, D_i^{(s)}$ defined in eq. (25) and (17) in the four schemes discussed in the text for the central values of the input parameters. The entries below the horizontal line correspond to using the AMM scheme, and varying the input parameters, one each at a time, fixing the rest to their central values.

	$D_t^{(d)}10^{-6}$	$D_u^{(d)}10^{-8}$	$D_t^{(s)}10^{-6}$	$D_r^{(d)}10^{-8}$	$D_i^{(d)}10^{-7}$	$D_i^{(s)}10^{-7}$
AMM	2.31	3.75	2.30	20.96	-2.34	-2.34
KS	2.12	2.18	2.11	1.42	-2.00	-2.05
LSW	2.40	5.16	2.39	32.59	-2.50	-2.43
HQET	2.14	2.88	2.13	-24.89	-1.99	-1.94
$m_b = 4.6\text{GeV}$	2.24	4.48	2.22	26.83	-2.31	-2.26
$m_b = 5.0\text{GeV}$	2.41	3.47	2.40	18.86	-2.39	-2.31
$m_t = 178.2\text{GeV}$	2.45	3.75	2.44	21.89	-2.36	-2.35
$m_t = 168.2\text{GeV}$	2.18	3.75	2.17	21.61	-2.33	-2.33
$\Lambda_{QCD}^{(5)} = 0.298\text{GeV}$	2.29	3.39	2.28	20.71	-1.97	-1.95
$\Lambda_{QCD}^{(5)} = 0.157\text{GeV}$	2.33	4.15	2.32	21.35	-2.70	-2.73

We now evaluate the theoretical precision in the determination of $\left|\frac{V_{td}}{V_{ts}}\right|$ from an eventual measurement of $\Delta\mathcal{R}$. The other uncertainties being insignificant, there are basically two sources of errors: (i) a small residual scale-dependence, and (ii) the LD-scheme-dependent uncertainty, which depends on the parameters ρ and η. In Fig. 5 we show the constraints on ρ and η from an assumed value of $\Delta\mathcal{R}$ with the LD-effects calculated in the AMM-approach. For each value of $\Delta\mathcal{R}$, the practically overlapping curves represent the effect of varying μ in the range $m_b/2 \leq \mu \leq 2m_b$. Numerically, the net μ uncertainty on the ratio $\Delta\mathcal{R}$ is found to be $\pm 0.6\%$. The effect of the errors of $m_t, \alpha_s(m_Z)$ and the b-quark mass are smaller and not shown.

The potentially largest uncertainty in $\Delta\mathcal{R}$, due to the LD-effects, is shown in Fig. 6, where we have plotted the constraints on ρ and η from assumed values of $\Delta\mathcal{R}$. The four curves shown correspond to the LD-schemes: AMM, KS, HQET and LSW. As remarked earlier, the LD-related uncertainty is vanishingly small for the central values of ρ and η, i.e. at or close to the apex of the drawn triangle. However, for other points in the (ρ, η)-plane, the uncertainty is perceptible but still small, except for regions of the (ρ, η)-plane which are already ruled out from the existing CKM fits.
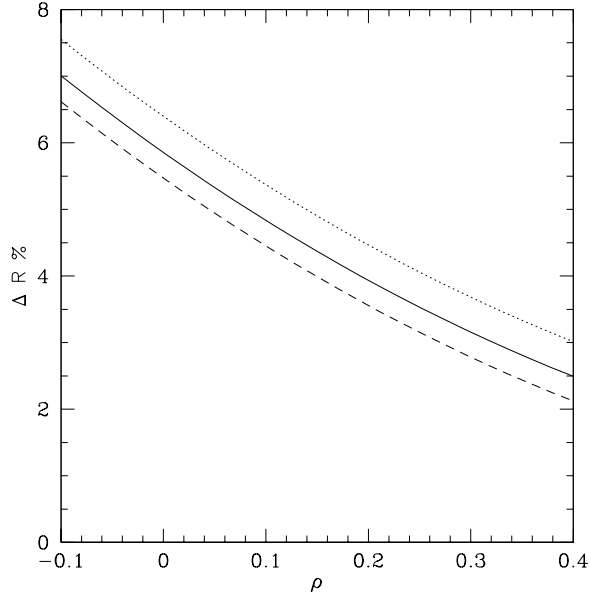
Figure 4: The ratio $\Delta\mathcal{R}$ defined in Eq. (24), calculated in the HQET-approach, as a function of ρ for three values of η; solid curve ($\eta = 0.383$), dotted curve ($\eta = 0.5$), dashed curve ($\eta = 0.27$).

4 Theoretical Precision on $|V_{td}/V_{ts}|$ from B Decays

The ratio $\Delta\mathcal{R}$ should be measurable at the Tevatron, the later phase of the B-factories, and certainly at the LHC. The merit of $\Delta\mathcal{R}$ lies in the theoretical precision on $|V_{td}/V_{ts}|$ (or on the unitarity triangle) which we have estimated here and found to be quite competitive with other proposals in the market, some of which are reviewed below.

The B^0-$\overline{B^0}$ mixing ratio $\Delta M_s/\Delta M_d$ can be expressed as follows:

$$\frac{\Delta M_s}{\Delta M_d} = \frac{M_{B_s}}{M_{B_d}} \frac{(f_{B_s}^2 \hat{B}_{B_s})}{(f_{B_d}^2 \hat{B}_{B_d})} |\frac{V_{ts}}{V_{td}}|^2 \ . \tag{27}$$

The achievable accuracy on V_{td}/V_{ts} depends, apart from the experimental measurement error, on the knowledge of the ratio of the hadronic matrix elements $\xi \equiv f_{B_d}\sqrt{B_{B_d}}/f_{B_s}\sqrt{B_{B_s}}$, for which the current Lattice estimate is $\xi = 1.14 \pm 0.06 \pm 0.03 \pm 0.10$ [3]. The errors reflect, respectively, the actual calculational error of this ratio in the quenched approximation, estimated effects of unquenching, and from chiral loops. Thus, the present theoretical error on this quantity is of $O(10\%)$ and it remains a theoretical challenge to improve this significantly. However, the measurement of ΔM_s, for which the present experimental lower bound is 12.4 ps^{-1} (at 95% C.L.)[33], may turn out to provide the first measurement of V_{td}/V_{ts}, as the central value of ΔM_s in the SM is around 14 ps^{-1} [32–34], which is not too far from the present limit.
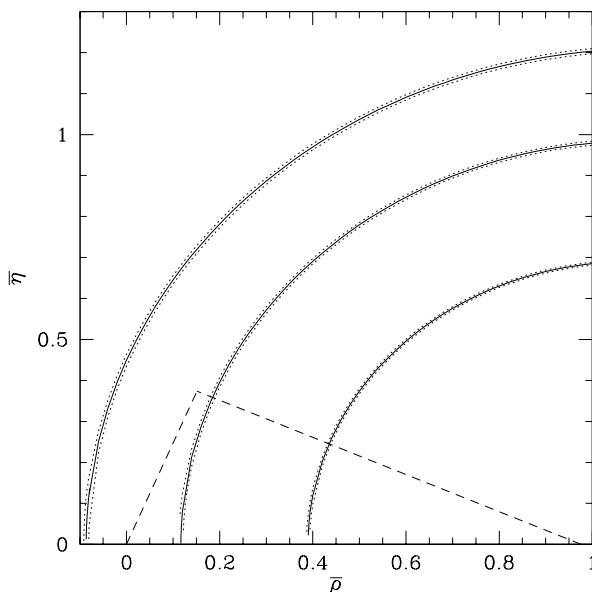
Figure 5: Contours in the $(\bar{\rho}, \bar{\eta})$ plane following from assumed values of the ratio $\Delta\mathcal{R}$; outer curve ($\Delta\mathcal{R} = 0.06$), central curve ($\Delta\mathcal{R} = 0.04$), inner curve ($\Delta\mathcal{R} = 0.02$). The overlapping curves for each value of $\Delta\mathcal{R}$ represent the uncertainty due to the renormalization scale. Also shown is the unitarity triangle corresponding to the central values of the CKM parameters from the analysis of Ref. [32].

Theoretical precision on $\Delta\mathcal{R}$ is comparable to the one on the corresponding ratio of the branching ratios involving the CKM-suppressed decay $B \to X_d + \gamma$ and the CKM-allowed decay $B \to X_s + \gamma$ [36,37]. Defining the ratio of the branching ratios as (implied are charge-conjugate averages)

$$R(d\gamma)/s\gamma) \equiv \frac{\langle \mathcal{B}(B \to X_d + \gamma)\rangle}{\langle \mathcal{B}(B \to X_s + \gamma)\rangle}, \tag{28}$$

the ratio $R(d\gamma)/s\gamma)$ gives a constraint on the CKM matrix elements which is very similar to the one given by $\Delta\mathcal{R}$ (compare Eq. (26) in Ref. [37] and Eq. (26) here). Theoretical error on $R(d\gamma/s\gamma)$ is estimated to be at most a few percent in [37], comparable to the one on $\Delta\mathcal{R}$. In hadronic collisions, the ratio $\Delta\mathcal{R}$ is more likely to be measured than $R(d\gamma/s\gamma)$.

We also mention here the exclusive radiative decays $B \to (\rho, \omega)\gamma$ and $B \to K^*\gamma$, whose ratios of the branching ratios can also be used to determine $|V_{td}/V_{ts}|$ [38]. The expected theoretical accuracy on the ratio $\mathcal{B}(B^\pm \to \rho^\pm + \gamma)/\mathcal{B}(B^\pm \to K^{*\pm} + \gamma)$ is, however, not anticipated to be better than $O(20\%)$ [39]. The corresponding LD-corrections in the ratios of neutral B-decays, $\mathcal{B}(B^0 \to (\rho^0, \omega) + \gamma)/\mathcal{B}(B^0 \to K^{*0} + \gamma)$ are expected to be smaller [39,40] due to their being both colour and (electric)-charge suppressed, hence
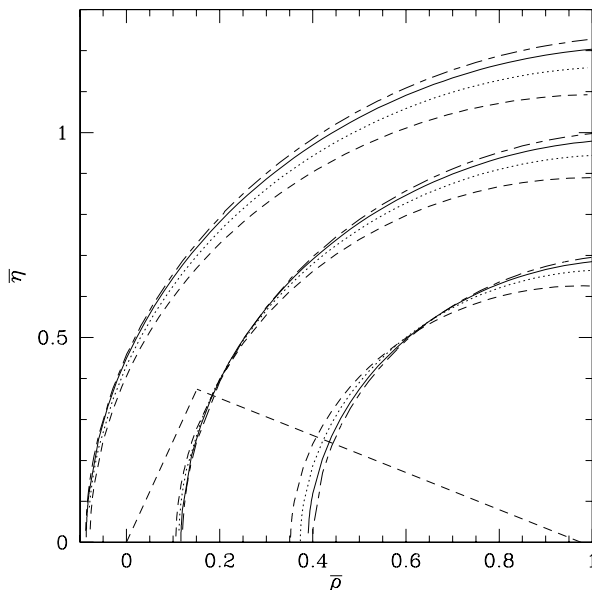
18

Figure 6: Contours in the $(\bar{\rho}, \bar{\eta})$ plane following from assumed values of the ratio $\Delta\mathcal{R}$; outer curve ($\Delta\mathcal{R} = 0.06$), central curve ($\Delta\mathcal{R} = 0.04$), inner curve ($\Delta\mathcal{R} = 0.02$). The solid, dotted, dashed, long-short dashed lines correspond to the AMM, KS, HQET and LSW approaches, respectively, for the central values of the parameters given in Table 1. Also shown is the unitarity triangle corresponding to the central values of the CKM parameters from the analysis of ref. [32].

reducing the theoretical uncertainty, but probably not better than $\pm 10\%$. Finally, we also note the constraints on $|V_{td}/V_{ts}|$, which can be obtained from the measurements of the ratios of some exclusive two-body non-leptonic decays, such as $\mathcal{B}(B^0 \to \overline{K^*}K^0)/\mathcal{B}(B^0 \to \phi K^0)$, advocated in Ref. [41]. This method may provide interesting results on the CKM ratio, but once data are available on the FCNC radiative and semileptonic decays discussed above, they are expected to provide more reliable information on the CKM matrix elements V_{td} and V_{ts}. In particular, the ratio $\Delta\mathcal{R}$ may provide one of the most precise determinations of $|V_{td}/V_{ts}|$.

We hope that the results presented here will help focus attention on experimental measurements of the branching ratios and CP asymmetries in the FCNC decays $B \to (X_d, X_s)\ell^+\ell^-$. We also underline the need to calculate the next-to-leading order corrections in the CP asymmetries to tame the scale dependence.

5   Acknowledgements

References

[1] N. Cabibbo, Phys. Rev. Lett. **10**, 531 (1963); M. Kobayashi and K. Maskawa, Prog. Theor. Phys. **49**, 652 (1973).

[2] M. Narain, in Proc. of the Seventh International Symposium on Heavy Flavors, Santa Barbara, Calif., 1997.

[3] T. Draper, hep-lat/9810065, to be published in the Proc. of the Conference Lattice '98, Boulder, Colorado, 1998.

[4] S. Adler et al. (E787 Collaboration), Phys. Rev. Lett. **79**, 2204 (1997).

[5] A. Ali, report DESY 97-256, hep-ph/9801270; to be published in Proc. of the Seventh International Symposium on Heavy Flavors, Santa Barbara, Calif., 1997.

[6] M.S. Alam et al. (CLEO Collaboration), Phys. Rev. Lett. **74**, 2885 (1995); T. Skwarnicki (CLEO Collaboration), in Proc. of the conference ICHEP'98, Vancouver, 1998.

[7] R. Barate et al. (ALEPH Collaboration), Phys. Lett. B **429**, 169 (1998).

[8] C. Caso et al. (Particle Data Group), Eur. Phys. J. **C3**, 1 (1998).

[9] A. Ali, C. Greub and T. Mannel, report DESY 93-016, ZU-TH 4/93, IKDA 93/5, published in the Proc. of the ECFA Workshop on a European B Meson Factory, Eds. R. Aleksan and A. Ali, Hamburg 1993.

[10] G. Buchalla, G. Isidori and S. -J. Rey, Nucl. Phys. B **511**, 594 (1998).

[11] G. Buchalla and A.J. Buras, Nucl. Phys. B **400**, 225 (1993).

[12] ALEPH Collaboration, Contributed paper (PA10-019) to the 28th. International Conference on High Energy Physics, Warsaw, 1996.

[13] We thank Peter Zerwas for bringing this to our attention. See also, the Proceedings of the Workshop on Physics and Detectors for a Linear e^+e^- Collider, Frascati, November 1998.

[14] C.S. Kim, T. Morozumi and A.I. Sanda, Phys. Rev. D **56**, 7240 (1997).

[15] A. Ali, L. T. Handoko, G. Hiller and T. Morozumi, Phys. Rev. D **55**, 4105 (1997).

[16] C.S. Lim, T. Morozumi and A.I. Sanda, Phys. Lett. B **218**, 343 (1989); N.G. Deshpande, J. Trampetic and K. Panose, Phys. Lett. B **214**, 467 (1988) Phys. Rev. D **39**, 1461 (1989); P.J. O'Donnel and H.K.K. Tung, Phys. Rev. D **43**, 2067 (1991).

[17] A. Ali, T. Mannel and T. Morozumi, Phys. Lett. B **273**, 505 (1991).

[18] A. Ali and E. Pietarinen, Nucl. Phys. B **154**, 519 (1979);
G. Altarelli et al., Nucl. Phys. B **208**, 365 (1982).

[19] A. Ali and G. Hiller, Phys. Rev. D **58**, 074001 (1998); D **58**, 071501 (1998).

[20] A. Ali and G. Hiller, preprint DESY 98-031, hep-ph/9807418 (submitted to Phys. Rev. D).

[21] D. Melikhov, N. Nikitin and S. Simula, Phys. Rev. D **57**, 6814 (1998); preprint hep-ph/9803343.

[22] F. Krüger and L.M. Sehgal, Phys. Lett. B **380**, 199 (1996).

[23] Z. Ligeti, I.W. Stewart and M.B. Wise, Phys. Lett. B **420**, 359 (1998).

[24] L. Wolfenstein, Phys. Rev. Lett. **51**, 1845 (1983).

[25] A.L. Kagan and M. Neubert, report CERN-TH-98-99, hep-ph/9805303.

[26] F. Krüger and L.M. Sehgal, Phys. Rev. D **55**, 2799 (1997).

[27] A. J. Buras and M. Münz, Phys. Rev. D **52**, 186 (1995).

[28] M. Misiak, Nucl. Phys. B **393**, 23 (1993) [E. B **439**, 461 (1995)].

[29] A. Czarnecki, M. Jeżabek and J. H. Kühn, Acta. Phys. Pol. B **20**, 961 (1989);
M. Jeżabek and J. H. Kühn, Nucl. Phys. B **320**, 20 (1989).

[30] A. J. Buras et al., Nucl. Phys. B **424**, 374 (1994).

[31] A.J. Buras, M.E. Lautenbacher and G. Ostermaier, Phys. Rev. D **50**, 3433 (1994).

[32] S. Mele, preprint hep-ph/9808411.

[33] F. Parodi, P.Roudeau and A. Stocchi, preprint hep-ph/9802289, and contributed paper # 586 to ICHEP '98, Vancouver, July 1998.

[34] A. Ali and D. London, Nucl. Phys. B (Proc. Suppl.) **54A**, 297 (1997), and to be published.

[35] S. Glenn et al. (CLEO Collaboration), Phys. Rev. Lett. **80**, 2289 (1998).

[36] A. Ali and C. Greub, Phys. Lett. B **287**, 191 (1992).

[37] A. Ali, H. Asatrian and C. Greub, Phys. Lett. B **429**, 87 (1998).

[38] A. Ali, V. Braun, and H. Simma, Z. f. Phys. C **63**, 437 (1994).

[39] A. Khodjhamirian, G. Stoll, and D. Wyler, Phys.. Lett. B **358**, 129 (1995); A. Ali and V. Braun, Phys. Lett. B **359**, 223 (1995).

[40] J.F. Donoghue, E. Golowich, and A.A. Petrov, Phys. Rev. D **55**, 2657 (1997).

[41] M. Gronau and J.L. Rosner, Phys. Lett. B **376**, 205 (1996).